

RESEARCH ARTICLE | JUNE 01 1964

## Vibrational Spectrum of Sodium Azide Single Crystals

James I. Bryant



*J. Chem. Phys.* 40, 3195–3203 (1964)

<https://doi.org/10.1063/1.1724984>



### Articles You May Be Interested In

Infrared Vibrations of Crystalline Potassium Azide

*J. Chem. Phys.* (June 1963)

Raman Spectrum of Potassium Azide Single Crystals

*J. Chem. Phys.* (August 1965)

Infrared Spectroscopic Investigation of Ultraviolet-Irradiated Sodium Azide Crystals

*J. Chem. Phys.* (April 1965)



Order now

Zurich  
Instruments

Freedom to Innovate.

The New VHFLI 200 MHz Lock-in Amplifier.

Orchestrate pulses, triggers, and acquisition as the hub of your experiment.  
Discover more – run every signal analysis tool, simultaneously.

## Vibrational Spectrum of Sodium Azide Single Crystals

JAMES I. BRYANT

*Basic Research Group, U. S. Army Engineer Research and Development Laboratories, Fort Belvoir, Virginia*

(Received 16 September 1963)

The infrared and Raman spectra of a single crystal of sodium azide have been intensively investigated at 298° and 90°K using grating spectrometers. Selection rules for internal and lattice vibrations are determined by application of the unit cell (factor group) method of Bhagavantam and Venkatarayudu. The unit cell modes of the crystal belonging to irreducible representations of the unit cell group have been constructed to within a good approximation. Spectra in the infrared are characterized by the occurrence of medium-strength absorptions symmetrically spaced about the principal bands of the spectrum with a separation of 122 cm<sup>-1</sup>. The observation of the Raman-active rotatory lattice mode at this frequency confirms the assignment of the medium-strength bands as sum and difference frequencies involving rotational motion of the azide ion as a rigid unit. Tentative assignments were made for all bands observed in the spectra and deduced frequencies for unobserved infrared lattice modes are presented. The spectra were found to be in good agreement with the accepted structure as described by the space group  $D_{3d}^5 - R\bar{3}m$ .

### I. INTRODUCTION

THE vibrational spectrum of sodium azide has been reported in the literature by several workers.<sup>1-6</sup> Most of these studies were made using samples in a powdered, mulled, or solution form. In the few cases in which single-crystal samples were used,<sup>5</sup> assignments were made primarily of fundamental modes and combinations thereof, with little or no consideration being given to spectral modifications occurring due to the presence of a crystalline field. The sodium azide crystal has a structure composed of relatively simple cell units which have been characterized by x-ray diffraction techniques. In addition, the symmetry, normal modes, and spectroscopic behavior of the free ion are well understood. These factors indicate that a vibrational study of single crystals of NaN<sub>3</sub> shows promise of yielding useful information concerning the motions and interactions of the ions in the crystal. The purpose of this study, therefore, was to carry out an intensive investigation of the infrared spectrum of single crystals of sodium azide between 4000 and 400 cm<sup>-1</sup>. Selection rules for the theoretically predicted vibrations are calculated using the "unit cell" method of Bhagavantam and Venkatarayudu.<sup>7,8</sup>

<sup>1</sup> W. G. Penny and G. B. Sutherland, Proc. Roy. Soc. (London) A156, 678 (1936).

<sup>2</sup> Delay, Duval and Lecompt, Bull. Soc. Chim. France 12, 581 (1945).

<sup>3</sup> L. Kohavec and K. Kohlrauch, Monatsh. Chem. 77, 180 (1947).

<sup>4</sup> P. Gray and T. Waddington, Trans. Faraday Soc. 53, 901 (1957).

<sup>5</sup> H. Papazian, J. Chem. Phys. 34, 1614 (1961).

<sup>6</sup> J. I. Bryant and G. C. Turrell, J. Chem. Phys. 37, 1069 (1962).

<sup>7</sup> S. Bhagavantam and T. Venkatarayudu, Proc. Indian Acad. Sci. A9, 224 (1939).

<sup>8</sup> S. Bhagavantam and T. Venkatarayudu, *Theory of Groups and its Application to Physical Problems* (Andhra University Press, Waltair, India 1951), p. 127-140.

### II. VIBRATIONS OF CRYSTALS

Halford<sup>9</sup> and Hornig<sup>10</sup> have shown that the number of vibrational frequencies allowed activity in infrared or Raman spectra can be calculated from the local symmetries of the molecules in crystals. However, as pointed out by Winston and Halford,<sup>11</sup> in order to obtain detailed information concerning the number, class, and symmetry species of lattice vibrations and their combination with fundamental vibrations, resort should be made to the "unit-cell" (factor group) method. The theory related to the development of the "unit-cell" method has been thoroughly treated elsewhere.<sup>7,8</sup> By application of the method, all the possible vibrations occurring in the unit cell of a crystal can be calculated and separated into classes which depend on the motion and vibrating species involved.

The total number of vibrations which can occur in a unit cell can be represented by the expression

$$\sum n_i = (1/N) \sum \sum h\rho \chi'_i(R) \chi(R), \quad (1)$$

where the symbols have their usual significance. Analytical expressions for the  $\chi(R)$  values have been derived by Bhagavantam and Venkatarayudu<sup>8</sup> and are reproduced for convenience in Table I. In this table,  $U_R$  is the number of atoms invariant under the symmetry operation  $R$  and the plus or minus sign is used according to whether  $R$  is a pure rotation through  $\Phi$  or a rotation through  $\Phi$  accompanied by a reflection. The letter  $s$  represents the sum of the number of groups of atoms and single atoms only occupying lattice points and  $v$  stands for the number of single atoms which occupy such sites.

<sup>9</sup> R. S. Halford, J. Chem. Phys. 14, 86 (1946).

<sup>10</sup> D. F. Hornig, J. Chem. Phys. 16, 1063 (1948).

<sup>11</sup> H. Winston and R. Halford, J. Chem. Phys. 17, 613 (1949).

TABLE I. Expressions for the character of the operation  $R$  for various vibrational classes.<sup>a</sup>

Vibrational class	Expression for the character of the operation $R$ , $\chi(R)$
Total vibrations of unit cell $\Sigma(n_i)$	$\chi(R) = U_R(\pm 1 + 2 \cos\Phi)$
Acoustic ( $T$ )	$\chi(R) = (\pm 1 + 2 \cos\Phi)$
Translatory ( $T'$ )	$\chi(R) = [U_R(s) - 1](\pm 1 + 2 \cos\Phi)$
Rotatory ( $R'$ )	$\chi(R) = U_R(s-v)(1 \pm 2 \cos\Phi)$
Internal ( $n'_i$ )	$\chi(R) = [U_R - U_R(s)](\pm 1 + 2 \cos\Phi)$ $- U_R(s-v)(1 \pm 2 \cos\Phi)$

<sup>a</sup> Reference 8, pp. 138-140.

### III. SYMMETRY AND VIBRATIONS

#### A. The Azide Ion

X-ray diffraction<sup>12</sup> and structural<sup>13</sup> studies indicate that the azide ion of sodium azide is linear and symmetric and hence belongs to the point group  $D_{\infty h}$ . Bassière,<sup>14</sup> however, has suggested that the ion is asymmetric in  $\text{NaN}_3$  with N-N bond lengths of 1.10 and 1.26 Å. This conclusion, in addition to conflicting with the above x-ray and structural results, is not supported by spectroscopic evidence.<sup>3-6</sup> In the present work, the symmetric structure is assumed correct. The point group  $D_{\infty h}$  gives rise to infrared activity for vibrations of species  $\Sigma_u$  and  $\Pi_u$ . The infrared spectrum of the "free" azide ion (as in a dilute gaseous system) thus consists of an asymmetric stretching vibration  $\nu_3$  and a doubly degenerate bending vibration  $\nu_2$ . The Raman-active symmetric stretching mode  $\nu_1$  completes the list of the four degrees of vibrational freedom. Only overtones and combinations of " $u$ " species are allowed activity in the infrared and these can conveniently be calculated using the  $u-g$  rule.

#### B. Sodium Azide Crystals

Sodium azide crystals are rhombohedral and belong to the space group  $D_{3d}^5$ — $\bar{R}\bar{3}m$ . The crystal structure is shown in Fig. 1. There is but one molecule per unit cell and all azide ions are aligned parallel with axes along the crystal's (111) zone axis. The "site" group for the azide ion in the crystal is therefore also  $D_{3d}$ . For the four atoms comprising the smallest cell, there are twelve degrees of freedom. The number of possible vibrations must also be equal to twelve and must fall within the six symmetry classes of the space group  $D_{3d}^5$ .

Quantities needed to determine the  $\chi(R)$  values are listed in Table II. For the  $\text{NaN}_3$  crystal structure with all azide ions aligned along the (111) zone axis of the

<sup>12</sup> S. Hendricks and L. Pauling, J. Am. Chem. Soc. **47**, 2904 (1925).

<sup>13</sup> L. Pauling, *The Nature of the Chemical Bond* (Cornell University Press, Ithaca, New York, 1944), p. 200.

<sup>14</sup> M. Bassière, Compt. Rend. **208**, 657 (1939); J. Chim. Phys. **36**, 71 (1939); Mem. Serv. Chim. État (Paris) **30**, 33 (1943).

crystal, there is no component of angular momentum in this direction. The quantity to be used instead of  $(1 \pm 2 \cos\Phi)$  in the expression for the character for rotatory vibrations in Table I can be selected from the three traces of the transformation matrices for rotation or reflection about the three crystal axes. These quantities are designated  $P(\Phi)$  and the expression for the rotatory character becomes

$$\chi(R) = U_R(s-v)P(\Phi). \quad (2)$$

When the symmetry operation involves a rotation about a given axis or a reflection through a plane perpendicular to the axis, the  $P(\Phi)$  value related to that axis is used. A more detailed description of the derivation and application of Eq. (2) can be found in Ref. 15.

The complete results of the application of the unit-cell method are presented in Table III. Since there is only one molecule per primitive cell, crystal-field splittings of fundamental absorptions do not occur. The basic spectrum is thus that of the dilute gaseous ion. However, two translatory and one rotatory lattice modes are allowed and these can combine with fundamentals to give lattice combinations which tend to modify considerably the features of the basic spectrum. Only vibrations of species  $A_{2u}$  and  $E_u$  are infrared active for the space group  $D_{3d}^5$  and the active fundamental and lattice combinations may be calculated using the usual multiplication properties of irreducible representations. Table IV lists the number of infrared-active lattice combinations which can occur about the

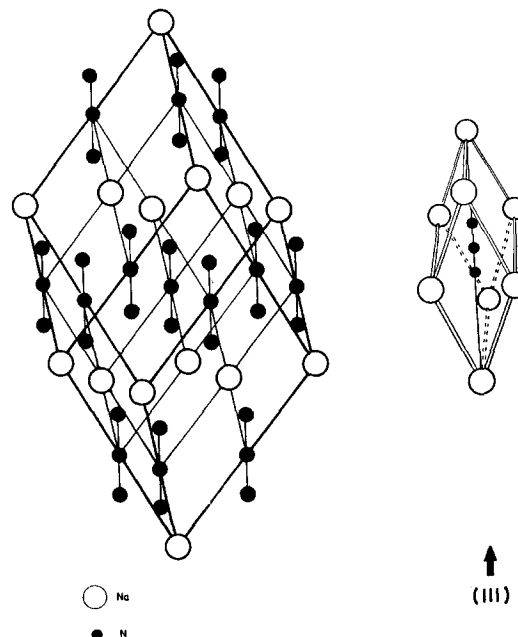


FIG. 1. Models of the structure and unit of structure of sodium azide single crystals.

<sup>15</sup> J. I. Bryant, J. Chem. Phys. **38**, 2845 (1963).

three fundamentals and the first overtone of the bending mode. These vibrations along with the active combinations between fundamental modes indicate the rapidity with which crystalline spectra can be complicated with structure.

The relative simplicity of the  $\text{NaN}_3$  unit cell suggested that the unit cell modes might be constructed within a good approximation. These constructions can conveniently be made in terms of the results of the application of the unit cell model and the definitions of the symmetry classes of the twelve predicted vibrations. The acoustic translational modes are represented as those in which all particles of a single cell move in the same direction, and the translatory (or optical) vibrations, those where the two types of particles move in opposite directions in such a manner that the center of gravity of each cell remains at rest. Rotatory lattice modes are represented as displacements resulting from the two or three degrees of rotational freedom of individual ions [in this case, a rotary oscillation or libration of  $\text{N}_3^-$  perpendicular to the (111) direction]. Figure 2 illustrates for a single primitive cell the unit

TABLE II. Quantities needed to calculate  $\chi(R)$  values for a single crystal of  $\text{NaN}_3$ .

Symmetry operation	$U_R$	$U_R(s)$	$U_R(s-v)$	$(\pm 1+2 \cos\Phi)$	$P(\Phi)$
$E$	4	2	1	3	2
$2C_3$	4	2	1	0	-1
$3C_2$	2	2	1	-1	0
$i$	2	2	1	-3	2
$2S_6$	2	2	1	0	-1
$3\sigma_d$	4	2	1	1	0

cell modes constructed for  $\text{NaN}_3$ . The arrows are intended to represent only the direction of displacement of given atoms and not magnitudes.

#### IV. EXPERIMENTAL

The crystals used in this study were grown from commercial  $\text{NaN}_3$ , raised to a high degree of purity by repeated reprecipitations. Flat transparent plates approximately 0.3 mm thick were obtained by very slow temperature reduction of aqueous solutions of the salt saturated at 56°C. In other cases, crystals up to 2 mm thick were grown by slow evaporation of aqueous solutions at 25°C. The thinnest crystals used (approximately 0.09 mm thick) were grown by a relatively rapid evaporation of solutions with depths not exceeding 1.5 mm.

Infrared spectra were measured using a Model 421 Perkin-Elmer Grating spectrometer over the frequency range from 4000 to 400  $\text{cm}^{-1}$ . The frequency accuracy specified for this instrument is  $\pm 1 \text{ cm}^{-1}$  and the resolution 0.3  $\text{cm}^{-1}$  at 2200 and 1000  $\text{cm}^{-1}$ . However, in this work this resolution was determined, by the study of gas-phase rotational lines, to vary from 0.5 to 0.8

TABLE III. Vibrational species of  $\text{NaN}_3$  single crystals.

$\mathfrak{D}_{3d}$	$\Sigma n_i$	$T_i$	$T_{i'}$	$R'$	$n_i'$	Activity
$A_{1g}$	1	0	0	0	1	$R \nu_1$
$A_{2g}$	0	0	0	0	0	
$E_g$	1	0	0	1	0	$R$
$A_{1u}$	0	0	0	0	0	
$A_{2u}$	3	1	1	0	1	$\text{IR } \nu_3$
$E_u$	3	1	1	0	1	$\text{IR } \nu_2$

$\text{cm}^{-1}$  throughout the spectral range covered. Spectra of most crystals were measured at 298 and 90°K with the sample mounted in a conventional low-temperature cell during both measurements. The 0.3 mm thick crystals produced spectra showing the most details throughout the complete spectrum, but it was necessary to use crystals of greater and lesser thicknesses to emphasize desired spectral features. Several replications were made of the spectrum of each crystal to increase the reliability of the data. Except in the orientation and polarization study mentioned below, crystals were mounted with the (111) zone axis approximately parallel to the incident beam of the spectrometer.

Since the azide ions of sodium azide are all aligned parallel in the crystal, orientations and polarization effects in the spectrum are expected to be pronounced. In aqueous solutions,  $\text{NaN}_3$  crystals tend to grow in thin plates with the azide ions perpendicular to the flat faces. When a crystal is mounted in the beam of the infrared spectrometer, the azide ions are all aligned essentially parallel to the incident beam and perpendicular to the plane of the  $E$  vectors (henceforth denoted as the parallel orientation). Thus any infrared vibrational species with symmetry about the axis of the azide ion ( $A_{2u}$  species) are inactive for this orientation of the crystal. The unit cell selection rules are thus modified by the above orientation of the crystal and only  $E_u$  species are allowed. However for crystals with any appreciable thickness,  $A_{2u}$  species vibrations can occur weakly, due to crystal imperfections, discrepancies in orientation, beam convergence, and combinations of these factors.

Efforts to study polarization effects were made using the 2 mm thick crystals. The edges of the best of these crystals were ground to a thickness of 1 mm with very

TABLE IV. Infrared-active binary lattice combinations of  $\text{NaN}_3$  single crystals.

Fundamental mode	Rotary combination bands	Translatory combination bands
$\nu_1$	0	4
$\nu_2$	4	0
$\nu_3$	2	0
$2\nu_2^a$	0	6

<sup>a</sup> Undergoes Fermi resonance with  $\nu_1$ .

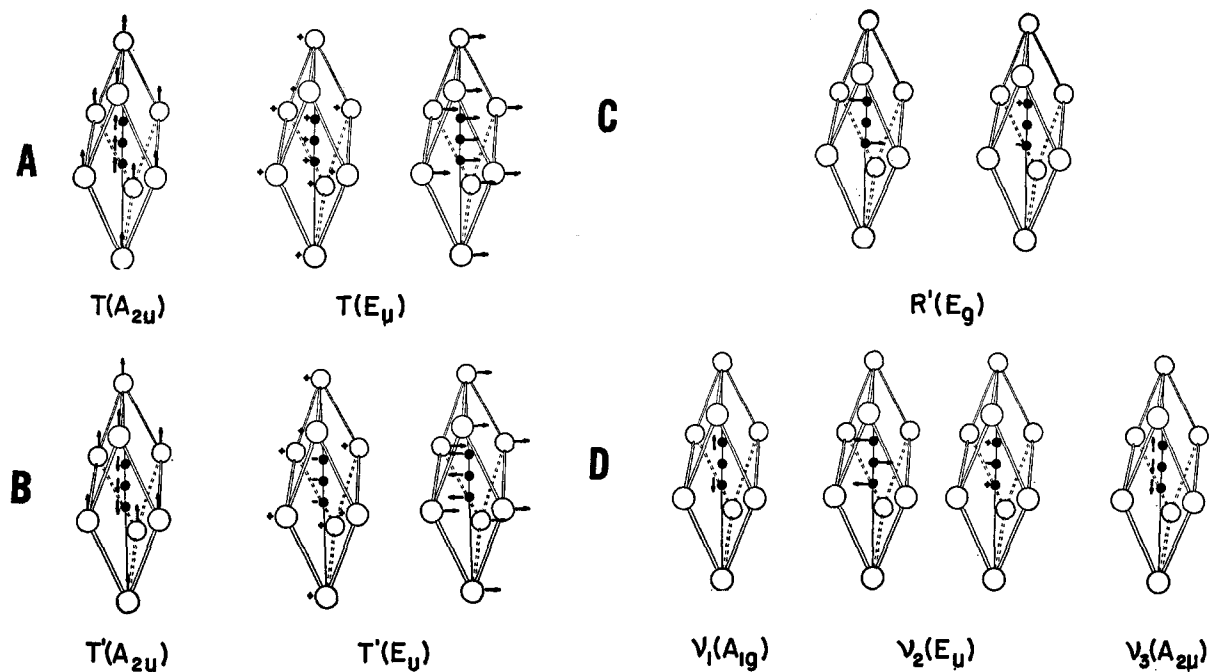


FIG. 2. Unit cell modes constructed for sodium azide: (A) acoustic; (B) translatory (optical); (C) rotatory; (D) internal.

fine abrasive paper and polished smooth on a jeweler's cloth moistened with acetone. By using crystals of this type, spectra could be measured with the (111) direction either parallel or perpendicular to the incident spectrometer beam by rotating the crystal through 90°. Due to the marked tendency of  $\text{NaN}_3$  to grow in thin plates, only one crystal was obtained which was thick enough to produce a useful spectrum when polarized infrared radiation was passed through the edge. Polarized infrared spectra of this crystal were measured in each of the two above orientations by orienting the polarizer to give maximum transmission and rotating the crystal through 180°. The polarizer used in this

work consisted of six plates of silver chloride mounted in a rectangular box at the Brewster angle. X-ray Laue photographs were recorded to check the internal structure of the crystal with respect to the external faces.

Raman spectra of the single-crystal samples were obtained with a Cary Model 81 Raman Spectrophotometer at the Applied Physics Corporation, Monrovia, California. The exciting radiation was the 4358-Å mercury line from a coil-type externally cooled Toronto arc. The spectra were measured with the sample mounted in a solid sample holder with the flat faces of the crystal perpendicular to the axis of the Toronto arc. Polarized spectra were measured by using cylindrical cross and axial polarizers. The accuracy of the reported Raman frequencies is estimated to be  $\pm 1 \text{ cm}^{-1}$ .

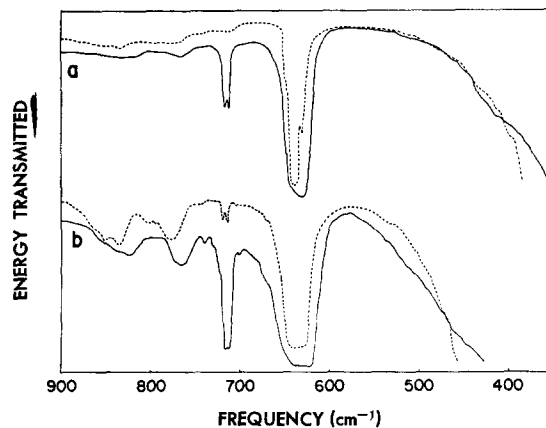


FIG. 3. Spectra of sodium azide single crystals in the  $\nu_2$  region: (a) 0.2 mm thick crystal. Solid line spectra were measured at 298°K and the broken line at 90°K; (b) 1.5 mm thick crystal.

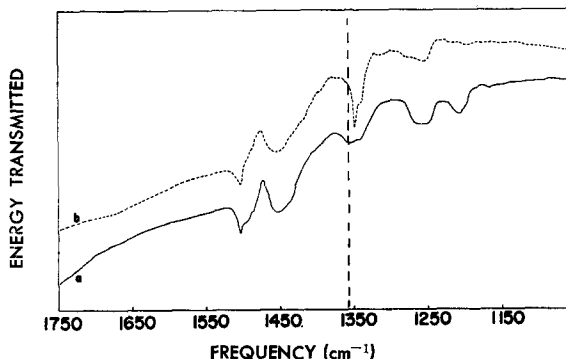


FIG. 4. Spectrum of 1.5 mm thick sodium azide single crystal in the symmetric stretching region: (a) 298°K; (b) 90°K.

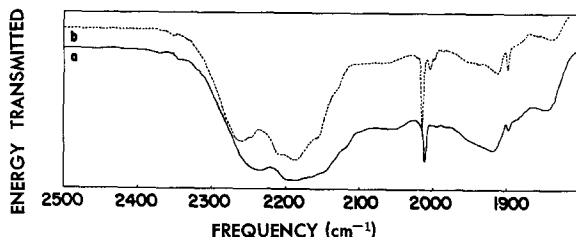


FIG. 5. Spectrum of 0.1 mm thick sodium azide single crystal in the asymmetric stretching region: (a) 298°K; (b) 90°K.

## V. RESULTS AND DISCUSSION

### A. Unpolarized Spectra

The vibrational spectrum of  $\text{NaN}_3$  crystals can conveniently be separated into parts as follows: the lattice vibration region ( $100\text{--}200\text{ cm}^{-1}$ ), the bending fundamental region ( $550\text{--}850\text{ cm}^{-1}$ ), the symmetric stretching region ( $1050\text{--}1550\text{ cm}^{-1}$ ), the asymmetric stretching region ( $1700\text{--}2350\text{ cm}^{-1}$ ), and the combination region near  $3300\text{ cm}^{-1}$ . Since no numerical calculations were made, assignments cannot be made with complete certainty. However, tentative assignments can be made based on the above selection rules and the experimental evidence obtainable. This includes the shape and intensity of bands, the agreement of frequencies for combination bands, the change of intensity and frequency with temperature, and the analyses of lattice combinations symmetrically arranged about active and inactive fundamentals. Even though the region of the infrared lattice vibrations is far beyond the frequency regions covered in this study, reasonable values for the frequencies occurring there could be inferred from lattice combinations.

The observed infrared spectra of  $\text{NaN}_3$  single crystals are presented in Figs. 3 through 6 and the Raman spectrum in Fig. 7. Polarized infrared spectra in the region of the bending fundamental are presented in Fig. 8. In the various regions investigated, all spectra which were used in making assignments have not been

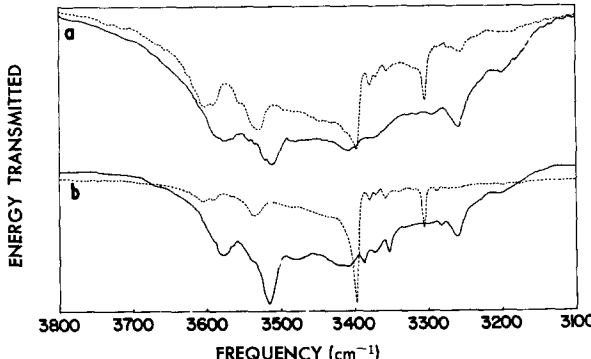


FIG. 6. Spectra of sodium azide single crystals in the 3300 wave-number summation region: (a) 0.8 mm thick crystal; 5 $\times$  ordinate scale expansion factor used; (b) 0.5 mm thick crystal; 10 $\times$  ordinate scale expansion factor used. Solid line spectra were measured at 298°K and the broken line at 90°K.

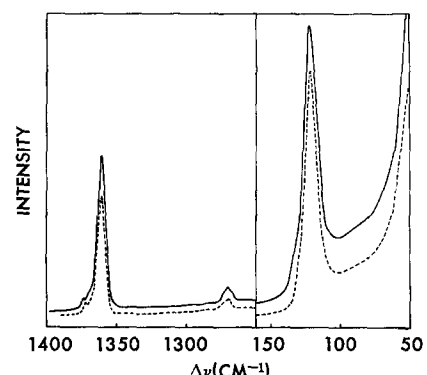


FIG. 7. Raman polarization spectra of  $\text{NaN}_3$  single crystal. The solid line spectrum was obtained using a cross polarizer and the dotted line spectrum, an axial.

presented here. Instead a spectrum was chosen which was determined to be most representative of the region concerned. The Raman spectrum of  $\text{NaN}_3$  single crystal shows three distinct bands, all of which are essentially depolarized. The line at  $122\text{ cm}^{-1}$  is the rotatory lattice mode  $R(E_g)$ , the only lattice frequency allowed Raman activity for the space group  $D_{3d}^5$  (see Table III). The strong line at  $1358\text{ cm}^{-1}$  is the sym-

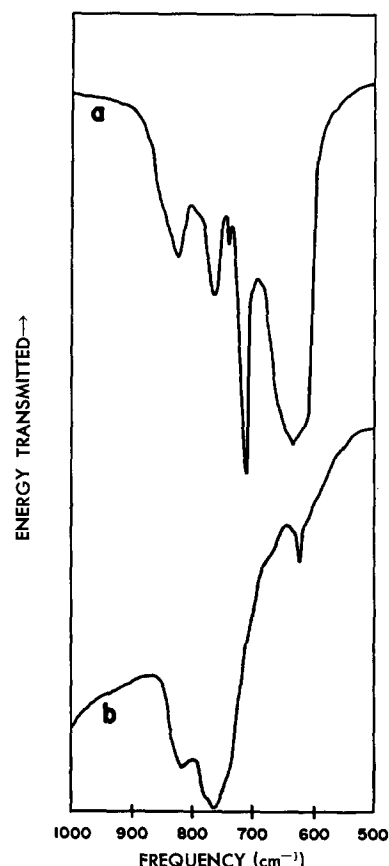


FIG. 8. Polarized infrared spectra of the  $\nu_2$  region of sodium azide crystal with the (111) direction perpendicular to the incident spectrometer beam: (a) polarization I; (b) polarization II.

TABLE V. Vibrational absorption of a single crystal of NaN<sub>3</sub>.

Frequency observed (cm <sup>-1</sup> )	Strength	Assignment	Remarks
122	s	$R'(E_g)$	Observed in Raman spectrum
530	vw?	$\nu_2 - R'(E_g)$	
628	w	$\nu_2$	Due to NaN <sup>15</sup> NN at natural abundance
638	vs	$\nu_2$	
708	w	$\nu_1 - \nu_2$	Due to <sup>15</sup> N isotope at natural abundance
713}	s	$\nu_1 - \nu_2$	Species $E_u$ , calc'd $\approx 712$ cm <sup>-1</sup>
716}	m	$\nu_2 + R'(E_g)$	
832	m	Second-order effect	
1208	w	$\nu_1 - T(A_{2u})$	$T(A_{2u}) \approx 150$ cm <sup>-1</sup>
1260	m	$\nu_1 - T(E_u)$	$T(E_u) \approx 98$ cm <sup>-1</sup>
1267	w	$2\nu_2$	Observed in Raman spectrum
1350	m	$\nu_1$	Due to NaN <sup>15</sup> NN at natural abundance
1358	s	$\nu_1$	Observed in Raman spectrum
1449	m	$\nu_1 + T(E_u)$	
1501	w	$\nu_1 + T(A_{2u})$	
1846	m	Second-order effect	
1898	w	$2\nu_2 + \nu_2$	Calc'd $\approx 1905$ cm <sup>-1</sup>
1920	s	$\nu_3 - R(E_g)$	
1995	w	$\nu_1 + \nu_2$	Species $E_u$
2011	m		
2043	m	$\nu_3$	
2166	s	$\nu_3 + R(E_g)$	
2235	s	Second-order effect	
2350	w	CO <sub>2</sub>	
3200	w	Second-order effect	
3182	vw	$(2\nu_2 + \nu_3) - R(E_g)$	
3262	m	$(\nu_1 + \nu_3) - R(E_g)$	
3306	s	$(2\nu_2 + \nu_3)[E_u]$	Frequency taken from pressed-disk spectra
3354	w	$(2\nu_2 + \nu_3)[A_{2u}]$	
3372	w	Second-order effect	
3389	w	Second-order effect	
3390	m	$\nu_1 + \nu_3$	Frequency taken from pressed-disk spectra
3415	m	$(2\nu_2 + \nu_3) + R(E_g)$	
3517	s	$(\nu_1 + \nu_3) + R(E_g)$	
3579	m	Second-order effect	

metric stretching fundamental  $\nu_1(A_{1g})$ . This mode undergoes only a slight Fermi resonance perturbation with the  $A_{1g}$  mode of the first overtone of the bending fundamental,  $2\nu_2$ . The resulting weak line due to the latter level appears at 1267 cm<sup>-1</sup>.

Beginning at the low-frequency end of the infrared spectrum, assignments are first made for the region of the bending fundamental  $\nu_2$ . Table III indicates that  $\nu_2$  is of species  $E_u$ . There is one lattice mode [ $R(E_g)$ ] capable of combining with  $\nu_2$  to give two infrared-active lattice combinations of species  $A_{2u}$  and  $E_u$ . Among the combinations which may occur in this region are  $2\nu_2 - \nu_2$ , of which there are three active species or components ( $A_{2u} + 2E_u$ ) and  $\nu_1 - \nu_2$ , which is of species  $E_u$ . The spectrum of the  $\nu_2$  region is shown in Fig. 3. Table V includes the list of assignments for this region.

The strong absorption centered at 638 cm<sup>-1</sup> is without doubt the bending fundamental  $\nu_2$ . In close proximity to  $\nu_2$ , at 628 cm<sup>-1</sup>, is a weak absorption which was observed only in thin crystals at low temperatures. The frequency of this band is assignable either as the combination  $2\nu_2 - \nu_2$  or as  $\nu_2$  due to the isotopic species NaN<sup>15</sup>NN present at natural abundance. Since the absorption became more highly resolved rather than less intense when the temperature was decreased to 90°K, the isotopic assignment is concluded to be the more feasible one. The frequency of  $\nu_2$  for the NaN<sup>15</sup>NN species was verified by direct observation in spectra of pressed KBr disk samples<sup>16</sup> containing NaN<sup>15</sup>NN<sup>17</sup> enriched to 95%. The strong "hot" band at 715 cm<sup>-1</sup> agrees well with the frequency of  $\nu_1 - \nu_2$  as calculated from the observed frequencies of the fundamentals. The apparent splitting of this absorption into a doublet is believed to be an example of the splitting of degenerate vibrations by crystal lattice vibrations as discussed by Hornig.<sup>10</sup> The medium strength absorption at 764 cm<sup>-1</sup> and the weak one at 741 cm<sup>-1</sup> can most reasonably be assigned as lattice combinations between the bending fundamental,  $\nu_2(E_u)$ , and  $R(E_g)$ . The difference between the frequency of the 764 band and the frequency of  $\nu_2$  agrees well with the Raman frequency  $R(E_g)$  occurring at 122 cm<sup>-1</sup> in Fig. 7. It is indicated later, from interpretations of polarized infrared spectra, that the 764 cm<sup>-1</sup> frequency can be assigned as the  $A_{2u}$  species of the lattice combination, and the 741 cm<sup>-1</sup> as the  $E_u$  species. Efforts to observe the infrared spectrum at frequencies beyond 500 cm<sup>-1</sup> were not successful. Even by using the 0.1 mm thick crystals, strong absorption due to lattice modes caused the transmission to begin to decrease rapidly at the above frequency and the crystal to become completely opaque at 400 cm<sup>-1</sup>. However, a weak doubtful absorption at approximately 530 cm<sup>-1</sup> was taken as the  $A_{2u}$  species of the difference

<sup>16</sup> M. Stimson and M. O'Donnell, J. Am. Chem. Soc. **74**, 1805 (1952).

<sup>17</sup> The <sup>15</sup>N-enriched azides were obtained from Hazelton Nuclear Science Corporation, Palo Alto, California.

band corresponding to the above-mentioned lattice combination.

The broad medium-intensity absorption at  $832\text{ cm}^{-1}$  exhibited temperature effects similar to the lattice combination at  $764\text{ cm}^{-1}$ , but could not be explained in terms of the unit cell selection rules. This and other similar absorptions are discussed after assignments for all regions of the infrared spectrum have been considered.

The infrared spectrum in the region of the symmetric stretching vibration is shown in Fig. 4 and the Raman shifts are displayed in Fig. 7. The unit-cell selection rules prohibit the occurrence of either  $\nu_1$  or  $2\nu_2$  in the infrared, but both are allowed in the Raman spectrum. The bands in this region in the infrared spectrum are due to lattice combinations with the Raman-active fundamental  $\nu_1$  affording an almost classical example of the so-called "forbidden" bands.<sup>9</sup> Two species of  $2\nu_2(A_{1g}+E_g)$  are also capable of combining with lattice modes to produce infrared bands in this region. However, due to the weak intensity of the  $2\nu_2$  absorption in the Raman spectrum, neither of the combinations with this mode are expected to be of sufficient intensity to be observed. Thus the lattice modes  $T'(A_{2u})$  and  $T'(E_u)$  are expected to combine with the  $A_{1g}$  species of  $\nu_1$  to produce active infrared absorptions in this region. In the observed infrared spectrum a group of medium intensity absorptions can be seen symmetrically situated about the Raman-active fundamental, indicated by the broken vertical line. The absorptions at  $1501\text{ cm}^{-1}$  and  $1208\text{ cm}^{-1}$  are assigned as the corresponding summation and difference bands, respectively, of  $\nu_1$  and a lattice mode of approximately  $150\text{ cm}^{-1}$ . Two somewhat more intense absorptions at  $1449\text{ cm}^{-1}$  and  $1260\text{ cm}^{-1}$  are similarly taken as the sum and difference, respectively, of the same fundamental and a lattice frequency of  $98\text{ cm}^{-1}$ . When the temperature was lowered from  $295^\circ$  to  $90^\circ\text{K}$ , all four of the absorptions underwent decreases in intensity and exhibited a slight shift outward from the position of the inactive fundamental. On the basis of the previously discussed intensity relations of  $A_{2u}$  and  $E_u$  species vibrations, the more intense absorptions at  $1260$  and  $1449\text{ cm}^{-1}$  can be assigned as  $E_u$  species bands and those at  $1208$  and  $1501$  as  $A_{2u}$  species. The band at  $1350\text{ cm}^{-1}$  exhibited no reduction in intensity, but became considerably sharper at low temperatures. It is believed to be the symmetric stretching vibration  $\nu_1$  due to the isotopic species  $\text{NaNN}^{15}\text{N}$  at natural abundance. The frequency observed for this mode in a  $\text{NaNN}^{15}\text{N}$ -enriched KBr disk sample was  $1351\text{ cm}^{-1}$ . A medium intensity band appeared in this region at  $1553\text{ cm}^{-1}$  when clean crystal surfaces were exposed to the atmosphere for periods greater than  $12\text{ h}$ . It could be essentially removed by polishing the faces of the crystal on a chamois moistened with acetone. This procedure removes the surface layer of the crystal faces and thereby the possible adsorbed water and

other surface impurities which apparently produce the absorption. It should be pointed out that spectra in this region were obtained using the  $5\times$  ordinate scale expander. On the normal 100% transmission scale of the spectrometer chart, the absorptions in this region were of the order of 10%. Therefore all are essentially "weak" intensity bands.

Figure 5 shows the region of the asymmetric stretching vibration  $\nu_3$ . This region is probably the most interesting of the spectrum, since it can illustrate the occurrence of possible misleading complications in single-crystal spectra. Since all azide ions are aligned parallel in the  $\text{NaN}_3$  crystal, when the flat crystals are mounted in the spectrometer, all  $\text{N}_3^-$  ions are essentially perpendicular to the plane of the  $E$  vectors of the incident beam. Thus, the normally intense (in an isotropic sample) fundamental is not expected to be highly absorbing in the spectrum since the  $\text{N}_3^-$  ions are oriented so that  $A_{2u}$  vibrations cannot interact appreciably with the incident beam. Only combination bands of  $E_u$  symmetry should appear with appreciable intensity in this region. In the observed spectrum, the band center of  $\nu_3$  was taken as  $2043\text{ cm}^{-1}$ . The two most intense bands in this region, which appear approximately  $122\text{ cm}^{-1}$  on either side of this frequency at  $2166$  and  $1920\text{ cm}^{-1}$ , are lattice combinations of  $\nu_3$  with  $R(E_u)$ . As expected from the Boltzmann factor, the summation band is more intense than the related difference band. Hornig<sup>10</sup> has pointed out that at sufficiently low temperatures, all combination bands must appear on the high-frequency shoulder of the fundamental. As the temperature is raised, the population of the upper lattice states will increase and as a consequence, difference bands will appear on the low-frequency shoulder. Such a tendency is shown in the  $\nu_3$  region as the sample temperature is lowered from  $298^\circ$  to  $90^\circ\text{K}$ . Superimposed on the broad envelope of  $\nu_3$  are sharp bands of medium to weak intensity which could confidently be assigned as the combinations  $\nu_1+\nu_2$  at  $2003\text{ cm}^{-1}$  and  $2\nu_2+\nu_2$  at  $1898\text{ cm}^{-1}$ . Finally, on the outer fringe of the  $\nu_3$  envelope are two broad medium-intensity bands at  $2235$  and  $1846\text{ cm}^{-1}$  which, like a similar absorption in the  $\nu_2$  region, could not be explained in terms of the unit-cell selection rules. These absorptions are discussed after assignments for the  $3300\text{ cm}^{-1}$  region are presented.

The last of the four infrared regions investigated contains the combination levels  $(\nu_1+\nu_3)[A_{2u}]$  and  $(2\nu_2+\nu_3)[A_{2u}+E_u]$  shown in Fig. 6. As was the case in the  $\nu_3$  region, the  $A_{2u}$  species of both  $(\nu_1+\nu_3)$  and  $(2\nu_2+\nu_3)$  are not expected to be strongly absorbing for the parallel orientation of the crystal. However, both  $(\nu_1+\nu_3)$  and  $(2\nu_2+\nu_3)$  are well resolved in the  $90^\circ\text{K}$  spectra at  $3400$  and  $3306\text{ cm}^{-1}$ , respectively, and were also easily observed as sharp bands in KBr pressed-disk samples where orientation is not a primary factor and the azide concentration is extremely low. The  $298^\circ\text{K}$  frequency values of  $3390$  and  $3299\text{ cm}^{-1}$

are taken as assignments for  $(\nu_1 + \nu_3)$  and  $(2\nu_2 + \nu_3)[E_u]$ , respectively, from the pressed-disk spectra. It is very likely that the broad absorption in the 298°K single-crystal spectra in the 3390 cm<sup>-1</sup> region is due to  $(\nu_1 + \nu_3)$ . A weak absorption at 3354 cm<sup>-1</sup> in the 298°K spectra of the single crystals is assigned as  $(2\nu_2 + \nu_3)[A_{2u}]$ . This weak absorption could also be clearly observed in the pressed-disk spectra. The remaining assignments in this region could be made from the 298°K single-crystal spectra. The strong absorption at 3517 cm<sup>-1</sup> and the medium-strength one at 3262 cm<sup>-1</sup> are assigned as the sum and difference of  $(\nu_1 + \nu_3)$  with the lattice frequency  $R(E_g)$ . Two less well defined bands at 3415 and 3182 cm<sup>-1</sup> are believed to be the sum and difference, respectively, of the same lattice frequency with the  $(2\nu_2 + \nu_3)$  combination. Weak absorptions on the low-frequency side of  $(\nu_1 + \nu_3)$  at 3389 and 3372 cm<sup>-1</sup> and  $(2\nu_2 + \nu_3)[E_u]$  at 3283 cm<sup>-1</sup> are probably evidence of the failure of the factor group selection rules to effectively describe combination and overtone transitions as pointed out by Mitra.<sup>18</sup> This investigator observed several bands for the first overtone of the internal mode of vibration of a brucite single crystal although the factor group selection rules predicted only one. It is interesting to note that the weak absorption at 3372 cm<sup>-1</sup> shows the expected frequency shift for  $(\nu_1 + \nu_3)$  due to NaNN<sup>15</sup>N at natural abundance. Finally, an anomalous absorption which could not be explained by the unit-cell selection rules is observed at 3579 cm<sup>-1</sup> on the high-frequency side of the 3517 cm<sup>-1</sup> lattice combination.

At this point, consideration will be given briefly to the previously mentioned absorptions which appeared in the various regions of the infrared spectrum but could not be explained by the unit-cell selection rules. These bands, which are loosely designated as second-order effects in Table V, all appeared on the outer fringe of the envelope of the absorption region in which they are found. Each band is separated by approximately 65 cm<sup>-1</sup> from a lattice combination band, and exhibits a temperature shift and a decrease in intensity identical to that of the lattice combination. Perhaps foremost among the explanations which we might consider for these bands is that they are due to splittings of the lattice combination, all of which are of species  $E_u$ . Hornig<sup>10</sup> has given theoretical consideration to the splitting of degenerate vibrations by crystal lattice vibrations and presents a table of symmetry types of vibrational modes which may be split which includes the lattice mode responsible for splitting. In this study, the suggested splitting would be of the order of 65 cm<sup>-1</sup>, which appears large, although splittings of approximately 50 cm<sup>-1</sup> have been reported for degenerate vibrations of CO<sub>3</sub> in calcite.<sup>10,19</sup> As an alternate and

equally feasible explanation for the unassigned bands, it might be suggested that they are analogous to multi-phonon absorptions observed in the spectra of numerous diatomic crystals. The use of the term phonon is not appropriate in this study since the azide ion is polyatomic. At present, very little is understood concerning second-order effects in spectra of polyatomic ions and considerable progress must be made experimentally before such absorptions can be observed and assigned with confidence.

## B. Polarized Spectra

Due to the unavailability of suitable samples, useful polarization spectra were obtained only for the region of the bending fundamental  $\nu_2$ . Polarized spectra in this region were measured with the (111) direction of the crystal oriented perpendicular (henceforth denoted as the perpendicular orientation) to the incident beam of the spectrometer. As expected from the symmetry of the unit cell, no polarization effects were observed for the parallel orientation [the (111) direction of the crystal parallel to the incident beam] of the crystal. Checks of the crystal's orientation by means of Laue photographs indicated that due to the convergence of the spectrometer beam, a fair amount of radiation always intersected the face of the crystal at angles other than 90°. For the perpendicular orientation, the intensity of  $\nu_2$  is several times greater than most of the remaining absorptions in the spectrum and the least convergence of the beam will produce this band with considerable intensity for any polarization. In addition, the thickness of the crystal used, coupled with the above-mentioned beam convergence, produced polarized spectra in the  $\nu_1$  and 3300 cm<sup>-1</sup> regions too poorly resolved to be useful. However, in the  $\nu_2$  region, definite intensity changes were observed, which could confidently be interpreted as polarization effects.

In this region, two mutually perpendicular polarizations produced spectra exhibiting the maximum intensity changes. It is likely that these polarizations represent alignments of the  $E$  vector with axes which are crystallographically significant. In Fig. 8, the bending fundamental [ $\nu_2(E_u)$ ], at 638 cm<sup>-1</sup>, decreases from a band of strong intensity in Spectrum (a) [polarization I] to one of negligible absorption in Spectrum (b) [polarization II]. This observation justifies the assignment of polarization I as one in which the  $E$  vector is essentially perpendicular to the crystal's (111) direction, and polarization II as one parallel to it. The combination band ( $\nu_1 - \nu_2$ ) at 715 cm<sup>-1</sup> is also of species  $E_u$  and underwent the same intensity changes as  $\nu_2$ . The medium-strength lattice combination [ $\nu_2(E_u) + R(E_g)$ ] at 764 cm<sup>-1</sup> and the absorption at 832 cm<sup>-1</sup> exhibited intensity changes just the reverse of those shown by  $\nu_2$  for the above two polarizations. On the

<sup>18</sup> S. S. Mitra, Solid State Phys. **13**, 1 (1962).

<sup>19</sup> C. Schaeffer and F. Matossi, *Das Ultrarote Spektrum* (Springer-Verlag, Berlin, 1930).

basis of this observation, the 764-cm<sup>-1</sup> band is assigned as the  $A_{2u}$  species lattice combination with  $\nu_2$ , and the weak lattice combination at 741 cm<sup>-1</sup> as the  $E_u$  species. The latter absorption appeared with very weak intensity for polarization I and vanished completely for polarization II.

#### ACKNOWLEDGMENTS

The author wishes to thank Dr. A. Maki and Dr. G. Wilmot for helpful discussions of this work. Thanks are also due to O. F. Kezer for providing some of the crystals used in this study. The cooperation and interest shown by Dr. Z. V. Harvalik are much appreciated.

## Self-Consistent-Field Theory. II. The LCAO Approximation

SERAFIN FRAGA AND FRASER W. BIRSS

*Department of Chemistry, University of Alberta, Edmonton, Alberta, Canada*

(Received 14 October 1963)

In Part I of this series, eigenvalue equations which apply to any electronic system were developed by means of a general coupling operator. These equations are here adapted to the method of linear combinations of atomic orbitals. The resultant matrix equations are applied to the helium atom for the configurations:  $^1S$ ,  $(1s)^2$ ;  $^3S$ ,  $(1s)(2s)$ ;  $^1S$ ,  $(1s)(2s)$ , using Slater  $1s$  and  $2s$  orbitals as basis functions.

### I. INTRODUCTION

IN Part I of this series<sup>1</sup> a method was developed for the treatment of self-consistent-field (SCF) problems which lays claim to general applicability in that no restrictions are made upon the number or the symmetry designation of possible open shells. It is well known that, in the absence of a central field, it is not possible, in general, to solve eigenvalue equations such as those that were given. Even where direct solution can be made the results must usually be expressed in a form which does not permit ready interpretation and application. Therefore, expansion of the orbitals in terms of a reasonable set of basis functions, and expression of the eigenvalue problem in terms of the expansion parameters, is normally employed.

In this paper we give the development in the context of the method of linear combination of atomic orbitals (LCAO). This is then applied to the cases  $^1S-(1s)^2$ ;  $^3S-(1s)(2s)$ ;  $^1S-(1s)(2s)$  of helium with a very small basis set.

The notation used in this paper depends very heavily on that given in I.

### II. LCAO EQUATIONS

The individual orbitals  $\phi_i^{\mu\alpha}$  are expanded in terms of a given set of suitable basis functions  $\chi_p^{\mu\alpha}$ :

$$\phi_i^{\mu\alpha} = \sum_p \chi_p^{\mu\alpha} C_{pi}^{\mu} = \chi^{\mu\alpha} \mathbf{C}_i^{\mu}, \quad (1)$$

where  $\chi^{\mu\alpha}$  is the *row* vector whose elements are the basis functions of symmetry designation  $\mu\alpha$ ;  $\mathbf{C}_i^{\mu}$  is the *column* vector with elements  $C_{pi}^{\mu}$ . The latter are inde-

pendent of subspecies designation, thus maintaining the correct symmetry transformation properties among the orbitals.

The orbitals are assumed to be orthonormal:

$$\langle \phi_i^{\mu\alpha} | \phi_j^{\mu\alpha} \rangle = \int \bar{\phi}_i^{\mu\alpha} \phi_j^{\mu\alpha} dV = \mathbf{C}_i^{\mu *} \mathbf{S}^{\mu\alpha} \mathbf{C}_j^{\mu} = \delta_{ij}, \quad (2)$$

where  $\mathbf{S}^{\mu\alpha}$  is the *overlap* matrix whose elements are

$$S_{pq}^{\mu\alpha} = \langle \chi_p^{\mu\alpha} | \chi_q^{\mu\alpha} \rangle = \int \bar{\chi}_p^{\mu\alpha} \chi_q^{\mu\alpha} dV. \quad (3)$$

(Although these elements are actually independent of subspecies designation, the complete symmetry labeling is maintained for consistency with the general notation.)

The eigenvalue equations, expressed in terms of the expansion vectors  $\mathbf{C}_i^{\mu}$ , are

$$\mathbf{R}^{\mu\alpha} \mathbf{C}_i^{\mu} = \theta_{ii}^{\mu\alpha} \mathbf{S}^{\mu\alpha} \mathbf{C}_i^{\mu}, \quad (4)$$

where  $\theta_{ii}^{\mu\alpha}$  is the eigenvalue, which is related to the orbital energy,  $\eta_i^{\mu\alpha}$ , by:

$$\eta_i^{\mu\alpha} = \theta_{ii}^{\mu\alpha} / f_i^{\mu}, \quad (5)$$

$f_i^{\mu}$  being the fractional occupancy of the  $i$ th shell of symmetry designation  $\mu\alpha$ .  $\mathbf{R}^{\mu\alpha}$  is the matrix representation of the operator  $R^{\mu\alpha}$  in terms of the basis set functions with elements:

$$R_{pq}^{\mu\alpha} = \langle \chi_p^{\mu\alpha} | R^{\mu\alpha} | \chi_q^{\mu\alpha} \rangle. \quad (6)$$

The operator  $R^{\mu\alpha}$  is defined by

$$R^{\mu\alpha} = \sum_k r_k^{\mu\alpha} \quad (7)$$

<sup>1</sup> F. W. Birss and S. Fraga, J. Chem. Phys. **38**, 2552 (1963).